Pertanika J. Sci. & Technol. **13(1)**: 31 - 42 (2005)
ISSN: 0128-7680

Static and Dynamic Analysis of Rockfill Dam Using Finite-infinite Element Method

[1]J. Noorzaei, [2]M. Karami, [1]Waleed A. Thanoon & [1]M. S. Jaafar
[1]Civil Engineering Department, Faculty of Engineering
Universiti Putra Malaysia, 43400 UPM, Selangor, Malaysia
[2]Post Graduate Student, Civil Engineering Department, Engineering College
University of Shahid Chamran, Ahvaz, Iran

Received: 5 May 2003

ABSTRAK

Dalam kertas ini, sebuah empangan dan tanah di bawahnya telah dimodelkan dengan menggunakan unsur tergabung terhingga-tak terhingga dalam keadaan terikan satah. Tegasan statik yang terjadi pada sistem empangan-asas disebabkan oleh beban-beban graviti dan hidrostatik telah dinilai. Analisis seismik kenyal-plastik sistem tersebut kemudiannya dilakukan dengan menggunakan kriteria Drucker-Prager untuk ketidakurusan bahan. Kesamaan gerakan diselesaikan melalui kaedah pengamiran tokokan masa Newmark. Kajian menekankan kelakuan struktur sistem empangan-asas yang dikenakan dengan gegaran gempa bumi. Kelakuan dalam bentuk kontur pesongan, agihan tegasan dan ragam kegagalan dibentangkan.

ABSTRACT

In this paper, the dam body and the underneath soil were modeled using coupled finite-infinite elements under plane strain conditions. Initially, static stresses developed in the dam-foundation system due to gravity and hydrostatic loads are evaluated. Elasto–plastic seismic analysis of the dam-foundation system is next carried out by adopting the Drucker-Prager criterion for the material nonlinearity. The equation of motion is solved by Newmark incremental time integration technique. The study focuses on the structural behaviour of the dam-foundation system under earthquake excitations. The behaviour in terms of displacement contours, stress distributions and the failure mode are presented.

Keywords: Finite-infinite elements, static, elasto-plastic seismic analysis

INTRODUCTION

The rockfill dam has been used in many parts of the world with increasing frequency in recent years. This type of the dam is one of the most attractive type for the consulting engineers because of its good adaptability, convenience of construction, good performance during the past earthquakes, safety and economy with the development of the technologies of construction and the application of new structural materials. Rock fill dams having different heights have been used in different parts of the world. As an example Kuzuryu dam which is 128 m high was constructed in Japan (Nose *et al.* 1980), Masjeid Soleyman dam which is 170 m high was built up in Iran (Jafarzadeh *et al.* 1998), and Messochara dam which is 150 m high was completed in Greece (Thanopoulos *et al.* 1998). To study the variation of stresses in the body of the dams subjected to static and dynamic loading, the finite element technique has been widely used.

Skermer *et al.* (1973) analysed a rockfill dam with impervious core using a three-dimensional finite element model. A hyperbolic model was used to account for material nonlinearity. The comparisons between the results obtained from the finite element analysis with the results measured in the rockfill dam at site showed good agreement. Seed *et al.* (1985) reported a set of conventional finite element analyses aimed at estimating the magnitude of sliding deformations of typical concrete faced rockfill dams subjected to base accelerations with a peak acceleration amplitude (PGA) of 0.5 g. It is concluded that in high seismic active area, the geometry of the dam body and abutments should be 1.6H :1V or flatter. Bureau *et al.* (1985) presented a study dealing with the seismic performance of rockfill dams in general and the possible modes of failure of concrete faced rockfill dams in particular. The permanent deformation obtained directly using DSAGE software is based on finite difference method. Sayed Khaleed *et al.*(1990) used incremental and interface elements to discretise the Cethana concrete-faced rockfill dam assuming plain strain condition.

Gazetas *et al.* (1992, 1995) have studied the 3D seismic response of an actual 120 m tall concrete-faced rockfill dam, and concluded that tall concrete-faced rockfill dams in narrow canyons of solid rock may experience extremely intense shaking at mid crest during strong seismic motions. Roa *et al.* (1996) studied the Santa Juana dam under static and earthquake excitation having peak acceleration of 0.3 g. The deformation in the dam body and stresses in the concrete slab are obtained using the finite element method. Mircerska *et al.*(1998) analysed a rockfill dam for linear and nonlinear cases using Process Software under plane strain condition. The linear and nonlinear behaviour of the dam in terms of displacement, acceleration and stress histories were presented and discussed.

In the present study which is the continuation of the author's previous work (Noorzaei *et al.* 1999, 2000, 2002) the material nonlinearity of Kavar rockfill dam have been taken into consideration by employing the Drucker Prager yield criteria. The behaviour of the dam with respect to accelerations, displacements and stresses in the dam body has been discussed. Moreover, an attempt has been made to find out the mode of failure in the dam.

Static and Dynamic Analysis

Static stresses developed in the dam-foundation system due to gravity and hydrostatic loads are evaluated using usual finite element procedure available in many finite element textbooks. The nonlinear dynamic analysis of rockfill dams involves the solution of the well-known dynamic Equation of motion (Zeinkeiwicz *et al.* 1972; Owen and Hinton 1980):

$$[M]\{\ddot{u}\} + [c]\{\dot{u}\} + [k]\{u\} = -[M]\{\ddot{u}_{(g)}\} \tag{1}$$

Using the Newmark step-by-step integration method the solution of Eqn. (1) can be expressed by:

$$\dot{u}_{t+\Delta t} = \dot{u}_t + [(1-\gamma)\Delta t]\ddot{u}_t + (\gamma\Delta t)\ddot{u}_{t+\Delta t} \quad (2)$$

$$u_{t+\Delta t} = u_t + (\Delta t)\dot{u}_t + [(0.5-\beta)(\Delta t)^2]\ddot{u}_t + [\beta(\Delta t)^2]\ddot{u}_{t+\Delta t} \quad (3)$$

The record of the earthquake is divided into definite steps and in each step, the displacement vector determined from which the strains and stresses at each time step are calculated.

Drucker–Prager failure criteria was used to investigate the yielding of the materials in the dam-foundation system using:

$$f = \alpha J_1 + \left(J_2^{'}\right)^{0.5} - K \quad (4)$$

where, J_1 and J_2' are first and second stress invariants,

$$\alpha = \frac{2\sin\phi}{\sqrt{3}\left(3-\sin\phi\right)} \quad \text{and} \quad K = \frac{6C\cos\phi}{\sqrt{3}\left(3-\sin\phi\right)}$$

At each time step, a check on material yielding is performed for all Gauss points using Eqn.(4). If the state of stress at a specific Gauss point exceeds the yielding stress, the effective stress and residual stress are calculated as:

$$\{\Delta f_r\} = \int_V [B]^T \{\sigma\} d_V - \{f_r\} \quad (5)$$

By comparing the effective stress with that obtained in the previous iteration, loading or unloading status at a specified Gauss point will be known. The portion of stress level that is greater than yield value must be brought back to the yield surface by iteration processes within each time step. This procedure is useful in earthquake analysis when accelerograms are used to characterise the ground motion when structural nonlinear effects are present.

ANALYSIS OF ROCKFILL DAM

Finite-Infinite Modeling

The numerical example selected to illustrate the structural behaviour of rockfill dam is the Kavar rockfill in southern part of Iran. The dam has been proposed and designed by the consulting engineers (Noorzaei *et al.* 1999, 2000). The Finite element discretisation of the dam-foundation system is shown in *Fig. 1.* The total number of the nodal points is equal to 533. The number of finite and infinite elements are 160 and 8 respectively. The software used for the analysis of the dam is a multi-element and general purpose two-dimensional finite element package developed by the author (Noorzaei *et al.* 2002). Appendix A shows the different types of elements such as eight-noded finite and five-noded infinite isoparametric element along with their shape function used for the idealization of the dam section. The berm in the upstream (shown in *Fig. 1*) has been added to enhance the stability of the dam. Different materials have been used for the main body of the dam and the berm.

Property	DamBody	Rock
$E_{dynamic}$ (MPa)	850	1000
E_{static} (MPa)	170	450
ν	0.3	0.25
C (MPa)	0.005	0.3
ϕ	45	40

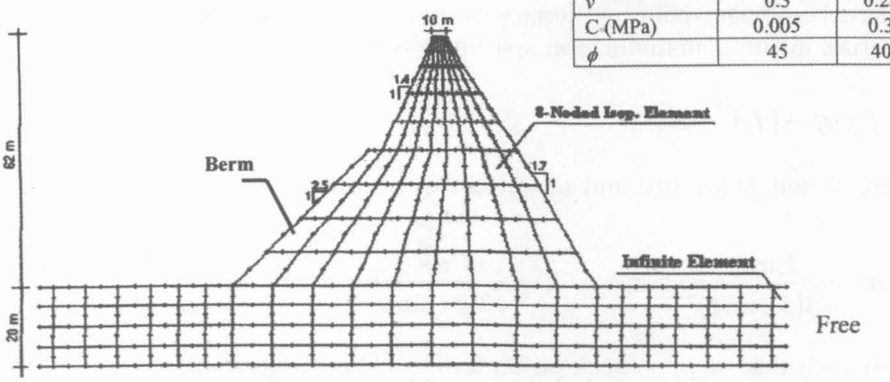

All the base node are fixed in both direction

Fig. 1: Finite-infinite element discretisation of rockfill dam

Static Analysis

Initially static analysis of the dam for the dead weight has been performed. The corresponding static stress vector and load vector are stored for the earthquake analysis of the dam. *Fig. 2* shows the contours of vertical and horizontal

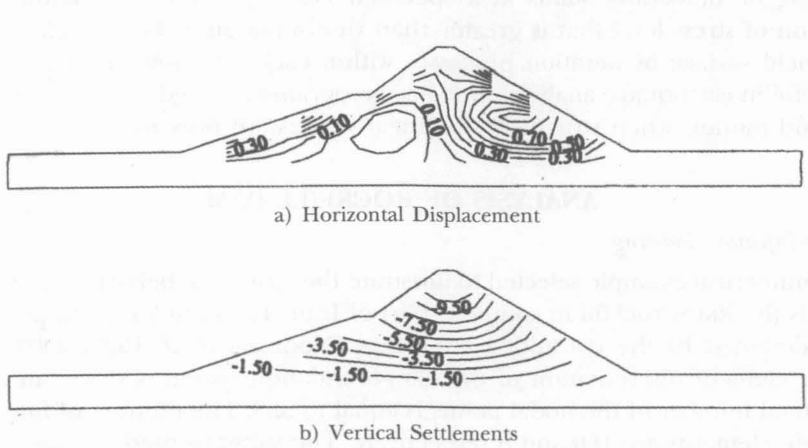

a) Horizontal Displacement

b) Vertical Settlements

Fig. 2: Contour lines of maximum horizontal and vertical settlement due to static load

settlements obtained form static analysis. The contours indicate that there is an increase in the vertical displacement as the height of the dam is increased and has a maximum value of 9.5 cm at the crest level of the dam. On the other hand, there is negligible movement in the horizontal direction.

The distributions of the static stresses throughout the body of the dam in term and the contours of maximum and minimum principle stresses are shown in *Fig. 3*. It is clear from this plot that highest values of principal stresses are developed at the centre of the lower portion of the dam and their values are decreasing with the increase of the height of the dam. The contours also show that both maximum and minimum principle stresses are in compression.

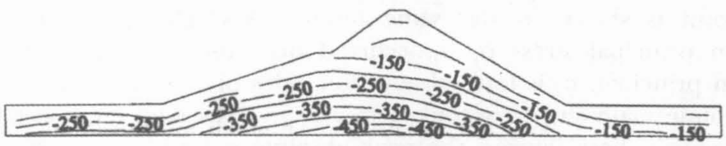

a) Maximum Principle Stresses

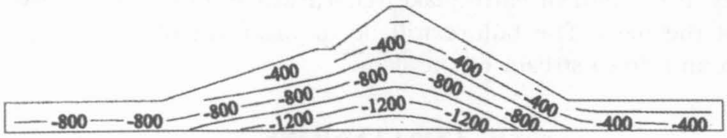

b) Minimum Principle Stresses

Fig. 3: Contour lines of maximum and minimum principle stresses due to static load

Dynamic Analysis

The dam-foundation system has been analysed for the earthquake excitation having PGA=0.27g and duration time equal 6.1 seconds [DBL record] as shown in *Fig. 4*. By using the direct Newmark integration technique, the record of earthquake is divided into 1220 steps. Damping of 5% has been assumed for the analysis.

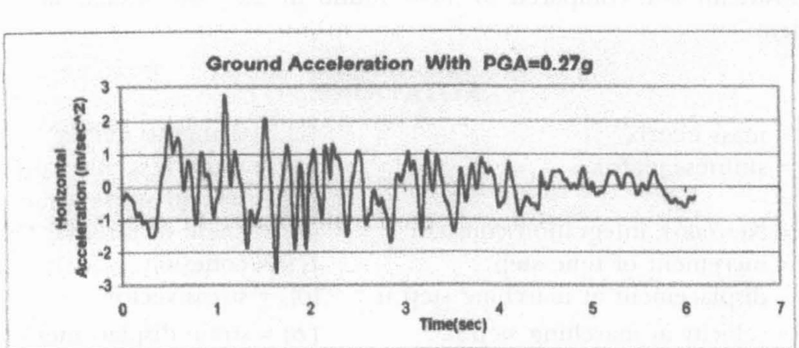

Fig. 4: Horizontal earthquake excitation record

The time history for the horizontal acceleration and displacement at three nodal points selected along the vertical central axis of the dam are shown in *Figs. 5* and *6* respectively. Node 204 is selected at the ground level while nodes 326 and 439 are chosen to be at the berm and crest level of the dam respectively. Both acceleration and displacement increase with the increase of the height of the dam. The absolute horizontal acceleration at the top of the dam is found to be 10.7 m/s^2, with an amplification factor (AF) of 3.96, while the peak absolute displacement at the top of the dam is found to be 3.03 centimeters.

Fig. 7 shows the time history of principle stresses and maximum shear stress at selected critical Gauss points in the dam section. The location of the selected Gauss point is shown in the same figure. This figure indicates that the maximum principal stress σ_1 is occurred near the ground level while the minimum principal, σ_3 is located at either sides of the dam. *Fig. 8* shows the peak absolute main stress contours (σ_1 , σ_3) in the dam cross-sections. As it can be seen in these figures, the peak absolute main stresses (σ_1 , σ_3) are mostly located at the foundation level. *Fig. 8* shows the plastification zone in the dam body at the end of earthquake record which also indicates the mode of failure of the dam. The failure will be in the form of wedges occurring at upstream and down stream of the dam.

CONCLUSIONS

The main conclusions that can be drawn from this work are:

(i) In static conditions, the maximum settlement occurred at the crest of the dam while the principal stresses reached their highest value in lower portions along the central core of the dam.

(ii) The damage of rockfill dam, resulting from earthquake, is in the form of wedge failure occurring upstream and downstream of the dam.

(iii) The maximum principal stress σ_1 occurred near the ground level while the minimum principal, σ_3 occurred at either sides of the dam.

(iv) The maximum and minimum main stresses are much higher in the upstream side compared to those found in the downstream side of the dam.

NOTATIONS

$[M]$	= mass matrix	$[c]$	= damping matrix
$[k]$	= stiffness matrix	J_1	= first stress invariants
α	=	J_2'	= second stress invariants
B	= Newmark integration constant	ϕ	= angle of internal friction
Δt	= increment of time step	C	= cohesion
U_n	= displacement at marching step n	$\{\sigma\}$	= stress vector
$\dot{u}_n$	= velocity at marching step n	$[B]$	= strain displacement matrix
$\ddot{u}_n$	= acceleration at marching step n	$\{f_r\}$	= external load vector
$\{\dot{u}\}_{t+\Delta t}$	= velocity at time $t+\Delta t$	$\{\Delta f_r\}$	= residual force vector

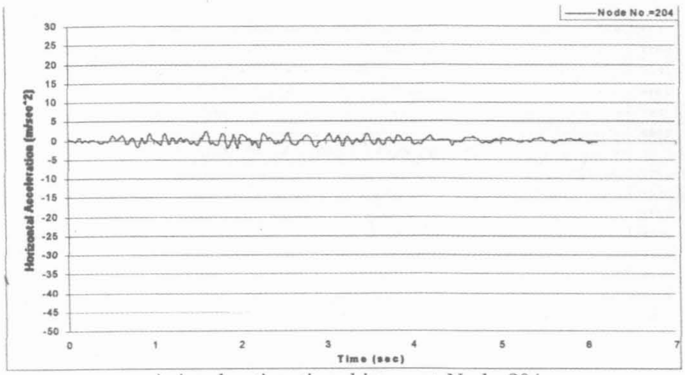

a) Acceleration time history at Node 204

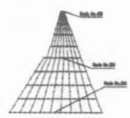

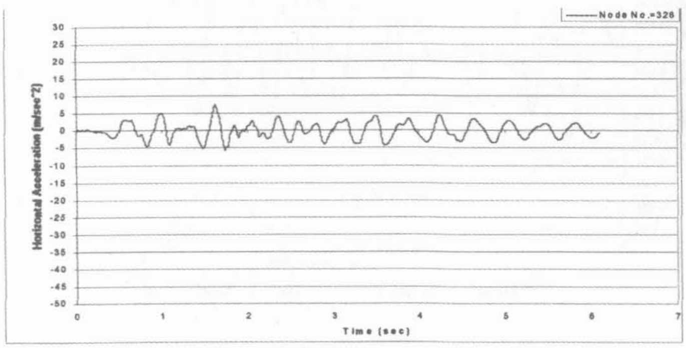

b) Acceleration time history at Node 326

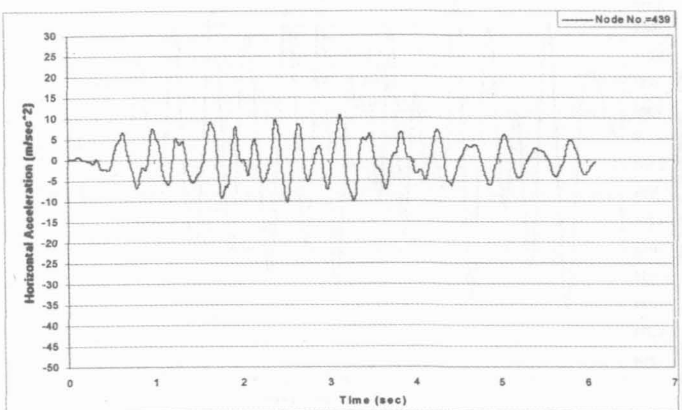

c) Acceleration time history at Node 439

Fig. 5: Horizontal acceleration at Node 204, 326 and 439

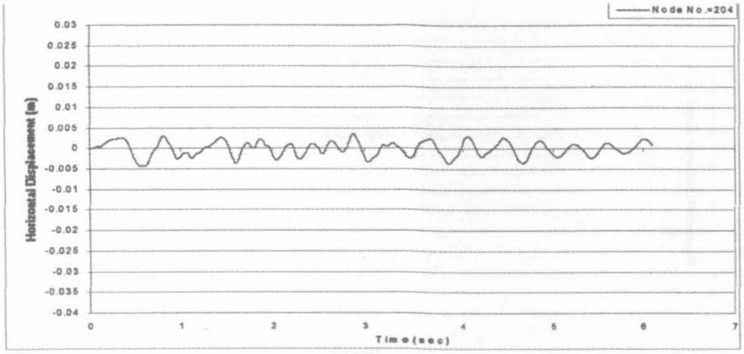

a) Displacement time history at Node 204

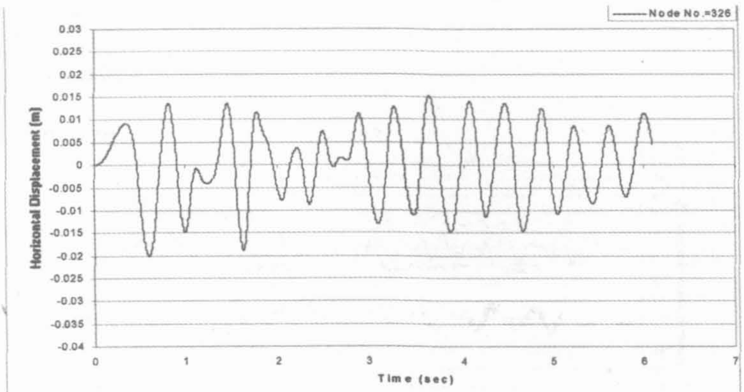

b) Displacement time history at Node 326

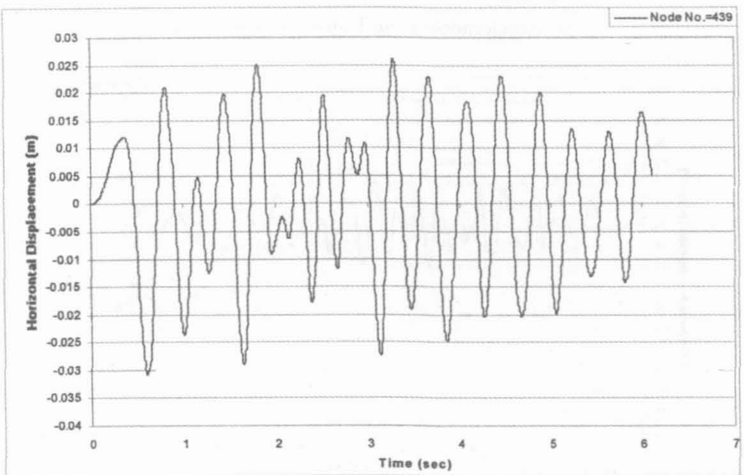

c) Displacement time history at Node 439

Fig. 6: Horizontal displacement at Node 204, 326 and 439

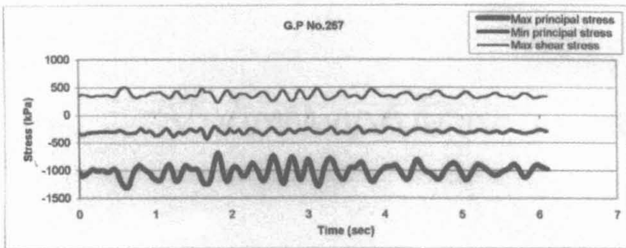

a) History of stresses in Gauss point No. 257

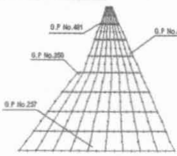

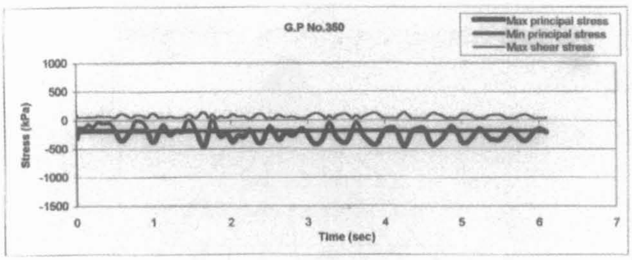

b) History of stresses in Gauss point No. 350

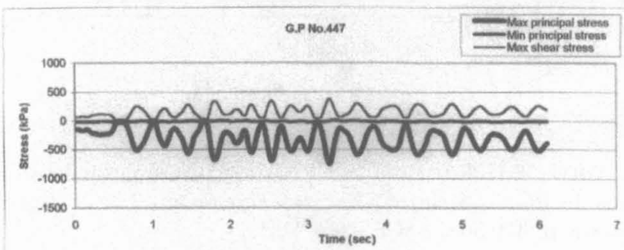

c) History of stresses in Gauss point No. 447

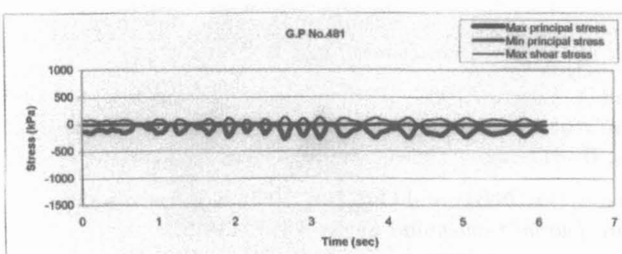

d) History of stresses in Gauss point No. 481

Fig. 7: Principle and shear stresses at critical G.P in the dam body

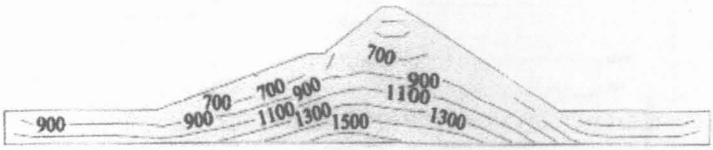

a) Minimum Principle Stresses

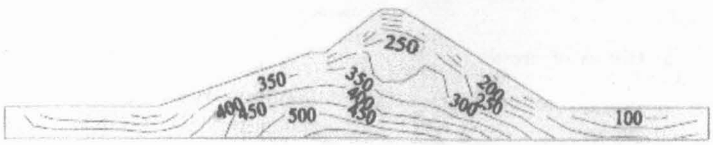

b) Maximum Principle Stresses

Fig. 8: Contours of peak absolute maximum and minimum principal stress (KPa)

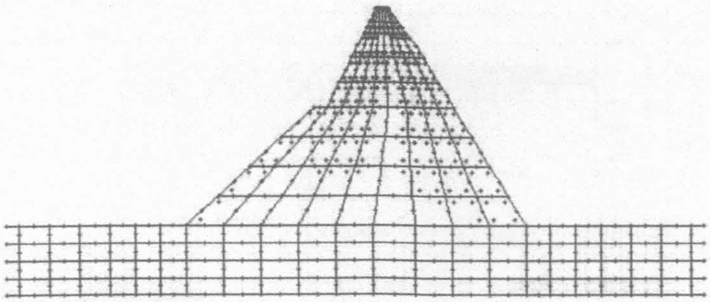

Fig. 9: Mod of failure

REFERENCES

BUREAU, G., R.L. VOLPE, W.H. ROTH and T. UDAKA. 1985. Seismic analysis of concrete face rockfill dams. In *Proc. of Symp. on Concrete – Face Rockfill Dams – Design, Construction, and Performance,* p. 479-508, ASCE, New York.

GAZETAS, G. and N. UDDIN. 1995. Dynamic response of concrete face rockfill dams to strong seismic excitation. *Journal of Geotechnical Engrg,* ASCE **121(2):** 185- 197.

GAZETAS, G. and P. DAKOULAS. 1992. Seismic analysis and design of rockfill dams: state of the art. *Soil Dynamic and Earthquake Engg.* **2:** 27-61.

JAFARZADA, F. and A. YAGHUBI. 1998. 3D dynamic behaviour of zoned rockfill dams with emphasis on real case study. In *Proced. Int. Symposium on New Trends & Guidelines on Dams Safety,* **II:** 817-824.

KHALID, S., B. SINGH, G.C. NAYAK and O.P. JAIN. 1990. Nonlinear analysis of concrete face rockfill dam. *Journal Geotechnical Engrg.* ASCE **116(5).**

MIRCEVSKA, V. and V. BICKOVSKI. 1998. Two-dimensional nonlinear dynamic analysis of rockfill dam. *Intenational Symposium on Dam Safety* **2:** 859-866.

NOORZAEI, J. and E. MOHAMMADIAN. 1999. Dynamic behavior of the Kavar CFRD in southern Iran. *Int Journal of Hydropower and Dams* **(6)**: 70-73.

NOORZAEI, J. and E. MOHAMMADIAN. 2000. Modeling of concrete face rockfill dam via finite-infinite and interface elements. In *Proc. Int. Symp. on CFRD*, p. 361-370, 18 Sept, Beijing.

NOORZAEI, J., M. KARAMI, T.A. WALEED and M.S. JAFAAR. 2002. Elasto-plastic seismic response of Kavar rockfill dam. In *12th International Symposium in Earthquake Engineering*, I.I.T, Roorkee, India, Dec. (To be presented).

NOSE M. and K. BABA. 1980. Dynamic behaviour of rockfill dams. In *Proceedings of Conference on "Dams & Earthquake"*, p. 69-78, Oct 1-2, London.

OWEN, D.R.J and E. HINTON. 1980. *Finite Elements in Plasticity: Theory and Practice*. UK: Pineridge Press Limited.

ROA, F.R. and L.A. GAMBOA. 1996. Seismic analysis of concrete – faced gravel-fill dams. In *Proceedings of the Int Symposium on Seismic and Environmental Aspects of Dams Design*, I, Santiago, Chile.

SKERMER, N.A. 1973. Finite element analysis of el infiernillo dam. *Can. Geotech. Journal* **10(2)**.

SEED, H.B., R.B. SEED, S.S. LAI and B. KHAMENEHPOUR. 1985. Seismic design of concrete – face rockfill dams. In *Proc of Symp. on Concrete-face Rockfill Dams – Design, Construction and Performance*, p.459-478, ASCE, New York.

THANOPOULOS, J. and J. TICOB. 1998. Erosion problems of concrete faced rockfill dams during construction. In *Proced. Int. Symposum on New Trends & Guidelines on Dams Safety*, **II:** 967-974.

ZIENKIEWICZ, O.C. and G.C. NAYAK. 1972. Elasto - plastic stress analysis, a generalization for various constitutive relation including strain softening. *Int Journal Num. Meth. Energy.* **5(1):** 113-135.

APPENDIX A

Shape functions for two-dimensional serendipity types of finite and infinite elements

Type of element	Element figure	Shape functions
Eight-nodes finite element	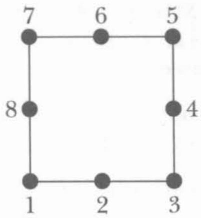	For corner nodes : $N_i = \frac{1}{4}(1+\xi\xi_i)(1+\eta\eta_i)(\xi\xi_i+\eta\eta_i-1)$ For midside nodes: a) $\xi = 0.0$ $N_i = \frac{1}{2}(1-\xi^2)(1+\eta\eta_i)$ b) $\eta = 0.0$ $N_i = \frac{1}{2}(1-\xi\xi_i)(1+\eta^2)$
Five-nodes infinite element	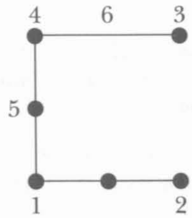	$N_1 = \frac{\xi\eta(1-\eta)}{(1-\xi)}$ $N_4 = \frac{-\xi\eta(1+\eta)}{(1-\xi)}$ $N_2 = \frac{(1+\xi)(1-\eta)}{2(1-\xi)}$ $N_5 = \frac{-2\xi(1-\eta^2)}{(1-\xi)}$ $N_3 = \frac{(1+\xi)(1+\eta)}{2(1-\xi)}$